

Structure, Transport and Magnetic properties in $\text{La}_{2x}\text{Sr}_{2-2x}\text{Co}_{2x}\text{Ru}_{2-2x}\text{O}_6$

P. S. R. Murthy^a, K. R. Priolkar^{a,*}, P. A. Bhoje^b, A. Das^c,
P. R. Sarode^a and A. K. Nigam^b

^a*Department of Physics, Goa University, Goa, 403 206 India.*

^b*Tata Institute of Fundamental Research, Homi Bhabha Road, Mumbai, 400 005
India*

^c*Solid State Physics Division, Bhabha Atomic Research Centre, Trombay, Mumbai
400 085 India*

Abstract

The perovskite solid solutions of the type $\text{La}_{2x}\text{Sr}_{2-2x}\text{Co}_{2x}\text{Ru}_{2-2x}\text{O}_6$ with $0.25 \leq x \leq 0.75$ have been investigated for their structural, magnetic and transport properties. All the compounds crystallize in double perovskite structure. The magnetization measurements indicate a complex magnetic ground state with strong competition between ferromagnetic and antiferromagnetic interactions. Resistivity of the compounds is in confirmation with hopping conduction behaviour though differences are noted especially for $x = 0.4$ and 0.6 . Most importantly, low field (50Oe) magnetization measurements display negative magnetization during the zero field cooled cycle. X-ray photoelectron spectroscopy measurements indicate presence of $\text{Co}^{2+}/\text{Co}^{3+}$ and $\text{Ru}^{4+}/\text{Ru}^{5+}$ redox couples in all compositions except $x = 0.5$. Presence of magnetic ions like Ru^{4+} and Co^{3+} gives rise to additional ferromagnetic (Ru-rich) and antiferromagnetic sublattices and also explains the observed negative magnetization.

Key words:

PACS: 72.15.Jf; 81.30.Kf; 75.50.Cc

* Corresponding author

Email address: krp@unigoa.ac.in (K. R. Priolkar).

1 Introduction

LaSrCoRuO₆ is a double perovskite whose magnetic properties critically depend on cationic order, charge balance and complex magnetic interactions between two transition metal ions [1,2,3]. Its crystal structure is composed of corner-shared CoO₆ and RuO₆ octahedra arranged in a pseudocubic array in the rocksalt arrangement. It is a semiconductor with ideal valence states HS Co²⁺ (3d⁷ high-spin configuration) and Ru⁵⁺ (4d³) [4]. Magnetically these compounds are reported to be antiferromagnetic with two magnetic face centered cubic (fcc) sublattices consisting of Co and Ru. Both the sublattices order with type II antiferromagnetic structure which would mean that the spins in [111] planes in succession Co-Ru-Co-Ru alternate as +/+/-/- . This marginalizes the Co-O-Ru nearest neighbor interactions and the ordering is governed by a competition between linear Co-O-Ru-O-Co and 90° Co-O-O-Co antiferromagnetic exchange paths [1,5]. The degree of ordering is known to affect the magnetic and transport properties due to changes in magnetic interactions and in cationic valence. Effects of anti-site disorder on the magnetic and transport properties due to La or Sr doping in LaSrCoRuO₆ have been investigated [1,5,6]. The change of composition (La or Sr doping) introduces mobile electrons in La richer samples or holes in Sr richer samples.

Another possible way of modifying magnetic and transport properties is by forming the solid solutions of antiferromagnetic LaCoO₃ and ferromagnetic SrRuO₃. These perovskite solid solutions of the form Sr_{1-x}La_xRu_{1-x}Co_xO₃ will have a strong interplay of cationic order, charge balance and complex magnetic interactions between the two B-site cations. In SrRuO₃ the 4d electrons of the low spin Ru⁴⁺ ions occupy the narrow π* band near Fermi level [7]. The lower 3d energy levels of Co³⁺ causes a charge transfer from 4d Ru⁴⁺ to 3d Co³⁺ [2]. However, Co can have various electronic states including high spin (HS) Co²⁺, Co³⁺ and Co⁴⁺, intermediate spin (IS) Co³⁺ and Co⁴⁺ and low spin (LS) Co³⁺ and Co⁴⁺ [8,9,10,11,12]. This complicates the situation giving rise properties like localized magnetic moment of Co [13], negative magnetoresistance [14]. In case of Sr_{1-x}La_xRu_{1-x}Co_xO₃, a complete charge transfer occurs at x = 0.5. At this composition the CoO₆ and RuO₆ octahedra align themselves in a pseudocubic array in the rocksalt arrangement forming the arch-type "double perovskite" structure.

The charge transfer between Ru and Co in LaSrCoRuO₆ is very sensitive to local atomic structure such as cation order [1,3,6]. Any disturbance in this cation order leads to compensation of antiferromagnetic interactions by the ferromagnetic interactions most likely associated with Ru-O-Ru interactions. The LaCoO₃ substituted SrRuO₃, has been known to exhibit large local magnetic moment arising due to Co spin polarizing the itinerant electrons of SrRuO₃ [2]. However, the delicate charge balance achieved in solid solutions by con-

version of Co^{3+} to Co^{2+} and oxidation Ru^{4+} to Ru^{5+} due to formation of double perovskite structure has not been addressed. More importantly the magnetic interactions at play as the system transforms from a ferromagnetic ground state to an antiferromagnetic one is far from being clearly understood. It is with this aim the present investigation is proposed. This paper describes detailed investigations carried out on the structural, magnetic and transport properties of solid solutions of SrRuO_3 and LaCoO_3 which form double perovskite compounds of the type $\text{La}_{2x}\text{Sr}_{2-2x}\text{Co}_{2x}\text{Ru}_{2-2x}\text{O}_6$, where $0.25 \leq x \leq 0.75$.

2 Experimental

Polycrystalline samples of $\text{La}_{2x}\text{Sr}_{2-2x}\text{Co}_{2x}\text{Ru}_{2-2x}\text{O}_6$, $0.25 \leq x \leq 0.75$ were synthesized by solid state reaction method by taking pre-dried stoichiometric amounts of La_2O_3 , SrCO_3 , $\text{Co}(\text{NO}_3)_2 \cdot 6\text{H}_2\text{O}$ and RuO_2 . These starting powders were ground thoroughly, pressed into pellets and heated for a total of 48 hrs, at 1300°C with three intermediate regrinding steps. All samples were deemed to be phase pure, as X-ray diffraction (XRD) data collected on a Rigaku X-ray diffractometer in the range of $18^\circ \leq 2\theta \leq 80^\circ$ using $\text{CuK}\alpha$ radiation showed no impurity reflections. The diffraction patterns were Rietveld refined using FULLPROF suite and structural parameters were obtained. DC magnetization (M) was measured, both as a function of temperature and magnetic field using the Quantum Design SQUID magnetometer (MPMS-5S). Magnetization as a function of temperature, $M(T)$ was measured in an applied field of 50 Oe and 1000 Oe in the temperature range of 5K to 300K. The sample was initially cooled from 300K to 5K in zero applied field and the data was recorded while warming up to 300K in the applied magnetic field (referred to as ZFC curve) and subsequent cooling (referred to as FC curve) back to 5K. Magnetization as a function of field was measured under sweep magnetic fields up to $\pm 5\text{T}$ at various temperatures. Before each $M(H)$ was recorded, the sample was warmed to 300K and cooled back to the desired temperature. Neutron diffraction (ND) measurements were performed at room temperature (RT) and 20K and a wavelength of 1.24\AA using powder diffractometer at Dhruva, Trombay. X-ray photoelectron spectra at Co (2p) and Ru (3d) levels were recorded using Thermo Fisher Scientific Multilab 2000 (England) instrument with $\text{Al K}\alpha$ radiation (1486.6 eV). The binding energies reported here is with reference to graphite at 284.5 eV having an accuracy of ± 0.1 eV.

Table 1

Expected (E) and refined (R) occupancies of Co and Ru for different values of $\text{La}_{2x}\text{Sr}_{2-2x}\text{Co}_{2x}\text{Ru}_{2-2x}\text{O}_6$.

$x \rightarrow$		0.25		0.4		0.5		0.6		0.75	
sites	atoms	E	R	E	R	E	R	E	R	E	R
$(\frac{1}{2}, 0, \frac{1}{2})$	Co	0.25	0.19	0.4	0.26	0.5	0.49	0.5	0.36	0.5	0.45
	Ru	0.25	0.31	0.1	0.24	–	0.01	–	0.14	–	0.05
$(\frac{1}{2}, 0, 0)$	Ru	0.5	0.44	0.5	0.36	0.5	0.49	0.4	0.26	0.25	0.20
	Co	–	0.06	–	0.14	–	0.01	0.1	0.24	0.25	0.30

3 Results

The Rietveld refined XRD patterns for all the compounds studied here are presented in Fig. 1. The samples crystallize in the $P2_{1/n}$ monoclinic structure with a initial increase followed by a decrease beyond $x = 0.5$ of cell volume as LaCoO_3 is added to SrRuO_3 to form a solid solutions. It may be mentioned here that the compounds with values of $x < 0.25$ and $x > 0.75$ have $Pbnm$ and $R\bar{3}c$ structures respectively and hence were not studied as they cannot be classified as double perovskites. Rietveld refinement of the XRD patterns were carried out with the $P2_{1/n}$ space group wherein the La/Sr occupy the 4e site with the fractional coordinates (0.00125,0.00774, 0.2463), Co is at 2c (0.5, 0, 0.5), Ru is at 2d (0.5, 0, 0) and the oxygen atoms occupy three sites, viz,(0.2491, 0.2566, 0.0295); (0.2207, -0.2233, 0.0295) and (-0.06418, 0.4995, 0.2507). The scale factor, back ground parameters, cell parameters, Co and Ru site occupancies along with instrumental broadening , totalling 17 parameters were refined in that order to obtain a good fit. As can be seen from Table 1 the B-site disorder was found to be least for $x = 0.5$ which also happens to be the stoichiometric double perovskite LaSrCoRuO_6 . Interestingly the disorder or the deviation from expected occupancy is highest for $x = 0.4$ and 0.6. This aspect needs more attention and perhaps magnetic and transport properties will shed light on this. The crystallographic parameters obtained from the above refinements along with the Curie-Weiss parameters calculated from magnetization measurements are all summarized in Table 2.

Magnetization measurements performed in applied fields of 1000 Oe and 50 Oe during the ZFC and FC cycles for $x = 0.25, 0.4, 0.6$ and 0.75 samples are presented in Fig. 2. In the case of $x = 0.25, 0.4$ and 0.6 there is a wide difference in magnetization recorded during the ZFC and FC cycles. The ZFC magnetization for these three samples, with increasing temperature increases sharply culminating into a broad hump centered around 50K. It decreases slightly with further rise in temperature before increasing sharply resulting in a peak at about 150K. The FC magnetization, on the other hand decreases

Table 2

Unit cell parameters obtained from Rietveld refinement and Curie-Weiss parameters calculated from magnetization measurements at 1000 Oe for $\text{La}_{2x}\text{Sr}_{2-2x}\text{Co}_{2x}\text{Ru}_{2-2x}\text{O}_6$. Numbers in parentheses are uncertainty in the last digit.

x	$a(\text{\AA})$	$b(\text{\AA})$	$c(\text{\AA})$	β°	$V(\text{\AA}^3)$	$\Theta_{CW}(K)$	$\mu_{eff}(\mu_B)$
0.25	5.5577(4)	5.5715(6)	7.8409(9)	90.05(2)	242.80(4)	62.8(2)	3.49(2)
0.40	5.5750(3)	5.5733(3)	7.8683(9)	90.25(2)	244.47(4)	49.5(2)	3.44(2)
0.50	5.5847(3)	5.5591(3)	7.8674(9)	90.05(2)	244.25(4)	-49.0(2)	3.87(2)
0.60	5.5626(3)	5.5287(3)	7.8245(9)	90.08(2)	240.63(4)	-20.8(2)	3.86(1)
0.75	5.4824(3)	5.5310(5)	7.7697(5)	89.93(3)	235.60(3)	-24.8(4)	3.82(1)

continuously to about 167K and then settles down into a low value giving an impression of a ferro to para transition. The wide difference in the magnetization between the ZFC and FC cycle indicates a complex magnetic ground state. It may also be noted that the magnetization (emu/mole) value at 5K decreases with increasing La and Co content. Further with increasing x the irreversibility between the ZFC and FC curves is also seen to decrease until at $x = 0.75$. For this composition there is a very little difference between ZFC and FC magnetization curves and the sample seems to order antiferromagnetically at $T_N = 34$ K.

The low field magnetization measurements are also in agreement with the above. The interesting point however is the observation of negative values of magnetization for three compositions viz, $x = 0.25, 0.4$ and 0.75 during ZFC cycle. Such negative values of magnetization were also seen in case of thermally disordered LaSrCoRuO_6 [3]. It may be noted here that all precautions were taken to ensure that negative values of magnetization are not due to remanent field of superconducting magnet of the SQUID magnetometer and this procedure has been described earlier [3]. Furthermore, as has been described later, the initial magnetization curves recorded for these samples at 5K also exhibit negative magnetization for lower values of field (see insets of Fig. 5). In case of $x = 0.75$ however, the magnetization was all along positive even during the ZFC cycle. The negative magnetization could be ascribed to presence of two magnetic sub-lattices which order in such a way as to cancel the magnetization of each other and in low fields align the net magnetic moment in a direction opposite to the applied field. The two magnetic sublattices could be conjunctured to be ferromagnetic $\text{Ru}^{4+}\text{-O-Ru}^{4+}$ and antiferromagnetic $\text{Co}^{2+}\text{-O-Ru}^{5+}$ and/or $\text{Co}^{3+}\text{-O-Co}^{3+}$.

This fact will be more clear from the values of effective paramagnetic moment μ_{eff} and Curie-Weiss temperature Θ_{CW} obtained from the high temperature magnetization behaviour. Curie-Weiss analysis has been employed to examine the behaviour of high temperature magnetization. The plots of the inverse

susceptibility ($1/\chi = H/M$) versus temperature are presented in Fig 3. For $x = 0.75$, the inverse susceptibility appears to vary linearly with temperature in the range $40\text{K} < T < 300\text{K}$ but a Curie-Weiss fit to the data indicates that there is a deviation from the linear fit below 160K . This is a characteristic progressive suppression of the spin-spin interactions as temperature decreases due to spin-orbit coupling [15]. The antiferromagnetic order below 34K can then be attributed to ordering of Co spins via non-magnetic $\text{RuO}_{6/2}$ bridges [16]. Therefore the data in the range $180\text{K} < T < 300\text{K}$ was fitted to the Curie-Weiss law and the values of μ_{eff} and Θ_{CW} were obtained. Likewise for all the other compounds too Curie-Weiss fitting was performed in the high temperature range (180K to 300K) and μ_{eff} and Θ_{CW} were calculated. These parameters are listed in Table 2. It can be seen that while the μ_{eff} varies only in a small range between 3.44 to $3.87 \mu_B$, Θ_{CW} shows a parabolic variation with x and changes its sign from negative for Co rich compounds to positive for Ru rich compositions. Negative Θ_{CW} indicates presence of stronger antiferromagnetic interactions while positive Θ_{CW} means stronger ferromagnetic interactions. In case of $x = 0.5$, the μ_{eff} value agrees very well with the calculated spin only moment value of Co^{2+} and Ru^{5+} indicating formation of a well ordered double perovskite. Another point to be noted is very large negative value of Θ_{CW} . This is an indicator of strong antiferromagnetic interactions and indeed this compound is reported to order antiferromagnetically at $T_N = 80\text{K}$ [1]. In other cases, the Ru rich compositions obviously have higher amount of $\text{Ru}^{4+}/\text{Ru}^{5+}$ leading to stronger ferromagnetic interactions and positive Θ_{CW} while the Co rich compounds have stronger antiferromagnetic interactions arising from higher amounts of $\text{Co}^{2+}/\text{Co}^{3+}$ ions. However, for all these compositions, μ_{eff} values reported in Table 2 can only be obtained by considering the presence of $\text{Ru}^{4+}/\text{Ru}^{5+}$ and $\text{Co}^{2+}/\text{Co}^{3+}$ redox couples. Even in case of $x = 0.75$ small deviation between ZFC and FC curves is seen below 160K (see Fig. 2). The presence of these magnetic ions results in formation of more than one magnetic sublattices giving rise to complex magnetic behaviour.

To establish the nature of magnetic order, ND patterns were recorded at low temperature (20K) and 300K for the two end members $x = 0.75$ and 0.25 . The Rietveld refined ND patterns at 300K for both these compounds are presented in Fig. 4. The parameters obtained from Rietveld refinement agree well with those obtained from XRD studies. The low temperature (20K) data shown in limited range in Fig. 4 indicates extra superlattice reflections due to antiferromagnetic ordering in $x = 0.75$. These reflections can be accounted for by an antiferromagnetic alignment of Co and Ru spins with a propagation vector along the $k = \frac{1}{2}, 0, \frac{1}{2}$ with respect to crystallographic axis. The magnetic arrangement is the same as determined for $x = 0.5$ in Ref. [1]. As per this model, the antiferromagnetic alignment is of type II which means that antiparallel spins are related by $(\frac{1}{2}, \frac{1}{2}, \frac{1}{2})$ translation operation. The refined spin moments for Ru and Co which were taken to be equal, were $\mu_x = 0.67(3)\mu_B$, $\mu_z = 0.36(6)\mu_B$ and resultant $\mu = 0.69(2)\mu_B$. No long range magnetic order

is visible in case of Ru rich composition ($x = 0.25$) indicating that the sharp rise in magnetization at about 160K is due to short range ferromagnetic correlations. The short range ferromagnetic correlations could be due to Ru-O-Ru linkages intervened by Co ions. These ferromagnetic correlations are present along with antiferromagnetic interactions as evidenced by the wide separation between ZFC and FC curves for this sample.

A further confirmation of the presence of competing magnetic interactions is obtained from isothermal magnetic response recorded for all the samples at various temperatures in the field range of ± 50 KOe. Fig. 5 presents the isothermal magnetization curves for four samples ($x = 0.25, 0.4, 0.6$ and 0.75) at 5K. It can be seen from this figure that for $x = 0.75$, the magnetization exhibits a strong field dependency and almost no hysteresis which is typical of an antiferromagnet. This is in agreement with antiferromagnetic ordering seen in M v/s T and ND measurements. On the other hand for all other compositions the isothermal magnetization exhibits a clear ferromagnetic hysteresis loop that rides on an antiferromagnetic (linear) background. Therefore the observed magnetic behavior can be ascribed to the presence of competing ferromagnetic and antiferromagnetic interactions. It is also noticed that with increase in Ru content, the area under the hysteresis loop increases implying the strengthening of ferromagnetic interactions. The initial magnetization curves shown as insets in Fig. 5 make it clear that the negative magnetization seen in the low field ZFC curves is indeed an intrinsic property of the materials studied here. Further it can also be seen that with the increase in x , magnetization turns positive at lower and lower values of applied field.

Presence of $\text{Co}^{2+/3+}$ and $\text{Ru}^{4+/5+}$ redox couples that give rise to complex magnetic behaviour will also affect the transport properties of the compounds. It may be mentioned here that while SrRuO_3 has metallic conductivity [17], LaCoO_3 exhibits semiconducting behaviour at temperatures below 300K [18]. A plot of ρ versus temperature for $\text{La}_{2x}\text{Sr}_{2-2x}\text{Co}_{2x}\text{Ru}_{2-2x}\text{O}_6$ with $0.25 \leq x \leq 0.75$ is presented in Fig.6. All the samples show semiconducting behaviour. It may be noted that the ordered composition ($x = 0.5$) has the highest magnitude of resistivity due to absence of any Ru-O-Ru type conducting paths. Since the resistivity of this ordered sample follows Mott's variable range hopping (VRH) behaviour, $\log \rho$ versus $T^{-1/4}$ has been plotted in the lower panel of fig. 6 for all compositions. It can be seen that along with $x = 0.5$, $x = 0.25$ and 0.75 samples show a linear behaviour indicating conduction to be in accordance with Mott's VRH law. Resistivity behaviour for $x = 0.4$ and 0.6 compounds however, is quite different. Here the ρ varies in a very narrow range and exhibits a hump at about 160K which coincides with the sharp rise in magnetization data of these samples. Rietveld analysis have also shown maximum B-site occupancy disorder for the same two compositions and therefore could be linked to the presence of more number of Ru-O-Ru conducting paths.

All the above properties hint at presence of $\text{Co}^{2+}/\text{Co}^{3+}$ and $\text{Ru}^{4+}/\text{Ru}^{5+}$ pairs in $\text{La}_{2x}\text{Sr}_{2-2x}\text{Co}_{2x}\text{Ru}_{2-2x}\text{O}_6$ compounds in different proportion. Core level XPS of Co and Ru can give an indication of valency of these ions and therefore a measure of such proportion. Fig 7 presents the background subtracted Co and Ru core level spectra for $x = 0.25, 0.5$ and 0.75 . Both Co $2p$ and Ru $3p$ spectra show two clear peaks due to spin orbit splitting and the associated satellite peaks (marked as *). In the case of Co, the main peaks are separated by a spin orbit splitting of about 15eV while in the case of Ru this splitting is about 22eV [19]. In the case of $x = 0.25$ and 0.75 , the main peaks are broadened as compared to $x = 0.5$ and show considerable spectral weight on the higher energy side especially in case of Co $2p$. Therefore the spectra have been fitted with two Gaussians perhaps corresponding to Co^{2+} and Co^{3+} species. Likewise the Ru $3p$ spectra also shows a presence of two types of Ru ions which are most likely to be Ru^{4+} and Ru^{5+} species. In case of $x = 0.5$, Co $2p$ and Ru $3p$ spectra can be well represented by a single gaussian which can be attributed to divalent Co and pentavalent Ru respectively. Further in case of $x = 0.25$ which has majority Ru content, the intensity of the peak corresponding to Ru^{4+} is higher than that of the peak corresponding to Ru^{5+} while the $x = 0.75$ sample shows higher amounts of Co^{3+} species as compared to Co^{2+} . This is as expected, the unexpected however is the corresponding contents of $\text{Co}^{2+}/\text{Co}^{3+}$ in $x = 0.25$ and $\text{Ru}^{4+}/\text{Ru}^{5+}$ in $x = 0.75$. Using the percentage concentration ratios of $\text{Co}^{2+}/\text{Co}^{3+}$ and $\text{Ru}^{4+}/\text{Ru}^{5+}$ obtained from area under the respective Gaussian's an attempt was made to calculate the spin only magnetic moments for the two compositions. The calculations were made assuming $S = 3/2$ for Co^{2+} and Ru^{5+} , $S = 1$ for Co^{3+} and $S = 2$ for Ru^{4+} . The calculated values were found to be $3.5\mu_B$ in case of $x = 0.75$ and $3.25\mu_B$ in case of $x = 0.25$. Although slightly lower, they seem to agree with the trend reported in Table 2.

4 Discussion

In the case of ordered double perovskite, LaSrCoRuO_6 , the presence of highly acidic Ru^{5+} stabilizes the high spin Co^{2+} and thereby suppressing various electronic transitions that Co ion can have. However, when the order is disturbed, Co-O-Co and Ru-O-Ru linkages are formed and the trivalent state of Co and tetravalent state of Ru are favoured. Such has been the case in $\text{La}_{2-x}\text{Sr}_x\text{CoRuO}_6$ [6].

In $\text{La}_{2x}\text{Sr}_{2-2x}\text{Co}_{2x}\text{Ru}_{2-2x}\text{O}_6$, present studies indicate that with the addition of LaCoO_3 to SrRuO_3 leads to stabilization of double perovskite phase is seen in a broad concentration region of $0.25 \leq x \leq 0.75$. These double perovskites, apart from $\text{Co}^{2+}\text{-O-Ru}^{5+}$ interactions will also contain Co-O-Co and Ru-O-Ru linkages. This is amply clear from the magnetic and transport proper-

ties described above. As mentioned above, these linkages favour trivalent and tetravalent states for Co and Ru respectively. Further, under such conditions it is well known that HS and IS states of Co^{3+} are promoted [20]. Presence of HS/IS Co^{3+} ions will give rise to additional magnetic interactions. Further $\text{Ru}^{4+}\text{-O-Ru}^{4+}$ is known to be ferromagnetic and metallic in conduction [21]. The observed competition between ferromagnetic and antiferromagnetic interactions can be therefore attributed to presence of Ru^{4+} and Co^{3+} ions. The presence of these ions along with occupancy disorder leads to formation of Ru rich and Co rich magnetic sublattices which order ferromagnetically and antiferromagnetically respectively. This is well supported by the decrease in magnetization values with increasing Co content and sharper rise of magnetization in case of Ru rich compositions. Only when there is a complete ordering of the B-site cations, Co^{2+} and Ru^{5+} ions are stabilized as nearest neighbours and long range antiferromagnetic order is established. The antiferromagnetic order seen in $x = 0.75$ can be attributed to antiferromagnetic cobalt ordering via non-magnetic $\text{RuO}_6/2$ bridges [16].

The presence of more than one magnetic sublattices also explains the negative magnetization observed in ZFC cycle of low field magnetization data. The ferromagnetic sublattice formed due to presence of tetravalent Ru ions orders at around 160K. This polarizes the paramagnetic Co spins in a direction opposite to the applied field leading to magnetic compensation and negative values of magnetization. With a decrease in Ru content, the ferromagnetic sublattice becomes weaker and the field required to reverse the magnetization to positive values also decreases. This can be very clearly seen from the initial magnetization curves presented in Fig. 5.

5 Conclusion

In summary, the structural, transport and magnetic properties in $\text{La}_{2x}\text{Sr}_{2-2x}\text{Co}_{2x}\text{Ru}_{2-2x}\text{O}_6$ have been studied. Double perovskite structure with space group $\text{P}2_{1/n}$ is stabilized over a wide composition range from $x = 0.25$ to 0.75. With the increase in Co content, ferromagnetic interactions are found to weaken and at $x = 0.75$ the compound orders antiferromagnetically at $T_N = 34\text{K}$. This interplay of ferromagnetic and antiferromagnetic interactions is attributed to presence of $\text{Ru}^{4+}/\text{Ru}^{5+}$ and $\text{Co}^{2+}/\text{Co}^{3+}$ redox couple in all the compounds. The only exception to this is the ordered compound $x = 0.5$ wherein Co and Ru exist in divalent and pentavalent states respectively representing an archtype double perovskite. The presence of different magnetic sublattices leads to magnetic compensation and negative magnetization. This can be explained by polarization of paramagnetic Co spins by the ferromagnetic Ru^{4+} sublattice in a direction opposite to applied field.

Acknowledgements

KRP and PRS would like to thank Department of Science and Technology (DST), Government of India for financial support under the project No. SR/S2/CMP-42. KRP and PSRM acknowledges support from UGC-DAE Consortium for Scientific Research, Mumbai Centre for financial support under CRS-M-126. Authors also thank Prof. M. S. Hegde for useful discussions.

References

- [1] J-W. G. Bos, J. P. Attfield, *Chem. Matter.* **16**, 1822 (2004).
- [2] A. Mamchik, W. Dmowski, T. Egami, I-W. Chen, *Phys. Rev. B* **70**, 104410 (2004).
- [3] P. S. R. Murthy, K. R. Priolkar, P. A. Bhoje, A. Das, P. R. Sarode and A. K. Nigam, *J. Magn. Magn. Mater.* **322** (2010) 3704.
- [4] D. Kim, B. L. Zink, F. Hellman, S. McCall, G. Cao and J. E. Crow, *Phys. Rev. B* **67**,100406 (2003).
- [5] Dlouhá M, Hejtmánek J, Jiráček Z, Knížek K, Tomeš P and Vratislav S 2009 *J. Magn. Magn. Mater.* doi:10.1016/j.jmmm.2009.06.035
- [6] P. Tomeš, J. Hejtmánek and K. Knížek, *Sol. State Sci.* **10**, 486 (2008).
- [7] G. Cao, S. McCall, M. Sheppard, J. E. Crow, R. P. Guertin, *Phys. Rev. B* **56** (1997) 321.
- [8] J. B. Goodenough, *J. Phys. Chem. Solids* **6** (1958) 287.
- [9] R. H. Potze, G. A. Sawatzky and M. Abbate, *Phys. Rev. B* **51** (1995) 11501.
- [10] T. Saitoh, T. Mizokawa, A. Fujimori, M. Abbate, Y. Takeda and M. Takano, *Phys. Rev. B* **55** (1997) 4257.
- [11] R. Caciuffo, D. Rinaldi, G. Barucca, J. Mira, J. Rivas, M. A. S. Rodriguez, P. G. Radaelli, D. Frorani and J. B. Goodenough, *Phys. Rev. B* **59** (1999) 1068.
- [12] P. G. Radaelli and S. -W. Cheong, *Phys. Rev. B* **66** (2002) 094408.
- [13] L. Pi, A. Maignan, R. Retoux and B. Raveau, *J. Phys: Condens. Matter* **14** (2002) 7391.
- [14] S. Manoharan, R. K. Sahu, D. Elefant and C. M. Schneider, *Solid State Commun.* **125** (2003) 103.
- [15] C. -Q. Jin, J. -S. Zhou, J. B. Goodenough, Q. Q. Liu, J. G. Zhou, L. X. Yang, Y. Yu, R. C. Yu, T. Katsura, A. Shatskiy, E. Ito, *Proc. Natl. Acad. Sci.* **105** (2008) 7115.

- [16] S. Kim, R. I. Dass and J. B. Goodenough, *J. Solid State Chem.* **181** (2008) 2989.
- [17] P. B. Allen, H. Berger, O. Chauvet, L. Forro, T. Jarlborg, A. Junod, B. Revaz and G. Santi, *Phys. Rev. B* **53** (1996) 4393; L. Klein, J. S. Dodge, C. H. Ahn, G. J. Snyder, T. H. Geballe, M. R. Beasley and A. Kapitulnik, *Phys. Rev. Lett.* **77** (1996) 2774.
- [18] P. M. Raccach and J. B. Goodenough, *Phys. Rev.* **155** (1967) 932; V. G. Bhide, D. S. Rajoria, G. R. Rao, and C. N. R. Rao, *Phys. Rev. B* **6** (1972) 1021.
- [19] J. F. Moulder, W. F. Stickle, P. E. Sobol, K. D. Bomben, *“Handbook of X-ray Photoelectron Spectroscopy”* (Physical Electronics, 1995)
- [20] K. Knížek, Z. Jiráček, J. Hejtmánek, P. Novák, *J. Phys.: Condens. Matter* **18** (2006) 3285.
- [21] I. I. Mazin and D. J. Singh, *Phys. Rev. B* **56** (1997) 2556.

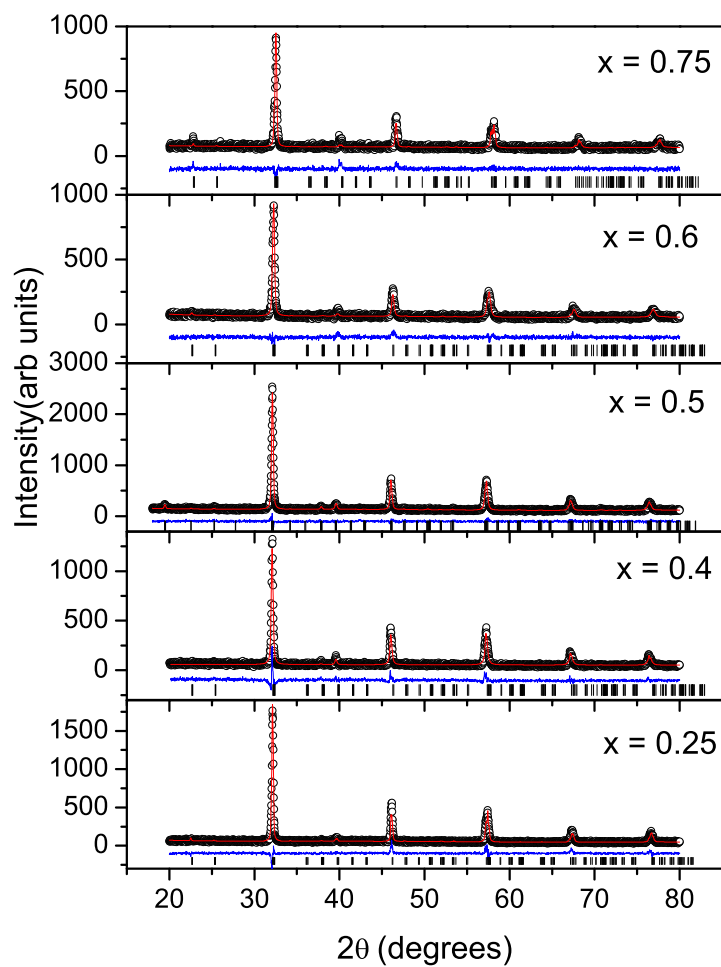


Fig. 1. Rietveld refined XRD patterns of $\text{La}_{2x}\text{Sr}_{2-2x}\text{Co}_{2x}\text{Ru}_{2-2x}\text{O}_6$. The open circles show the observed counts and the continuous line passing through these counts is the calculated profile. The difference between the observed and calculated patterns is shown as a continuous line at the bottom of the two profiles. The calculated positions of the reflections are shown as vertical bars.

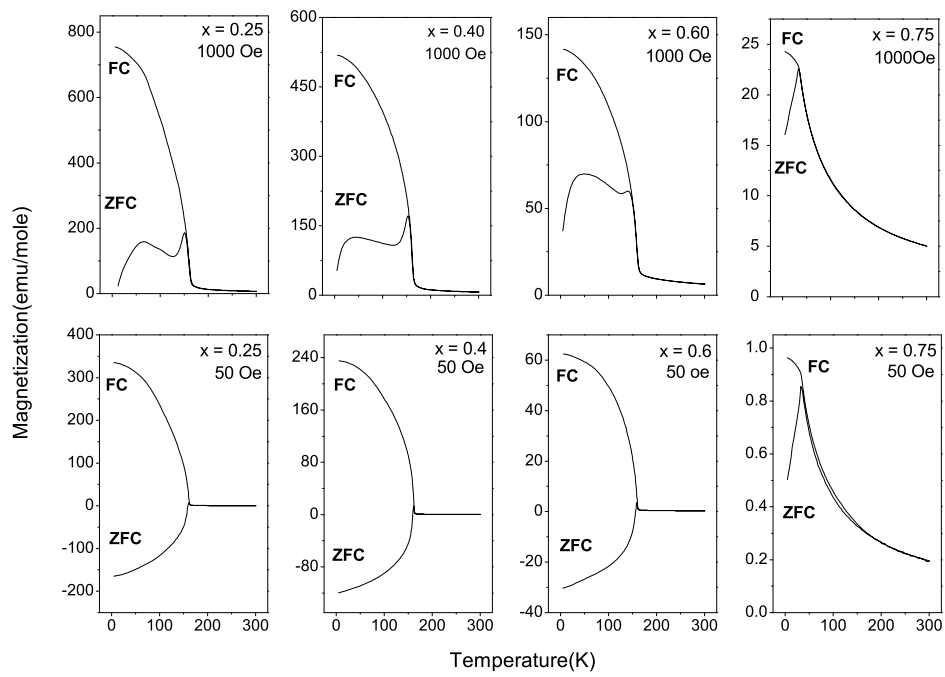


Fig. 2. Magnetization as a function of temperature recorded in applied fields of 1000 Oe (upper panel) and 50 Oe (lower panel) in $\text{La}_{2x}\text{Sr}_{2-2x}\text{Co}_{2x}\text{Ru}_{2-2x}\text{O}_6$.

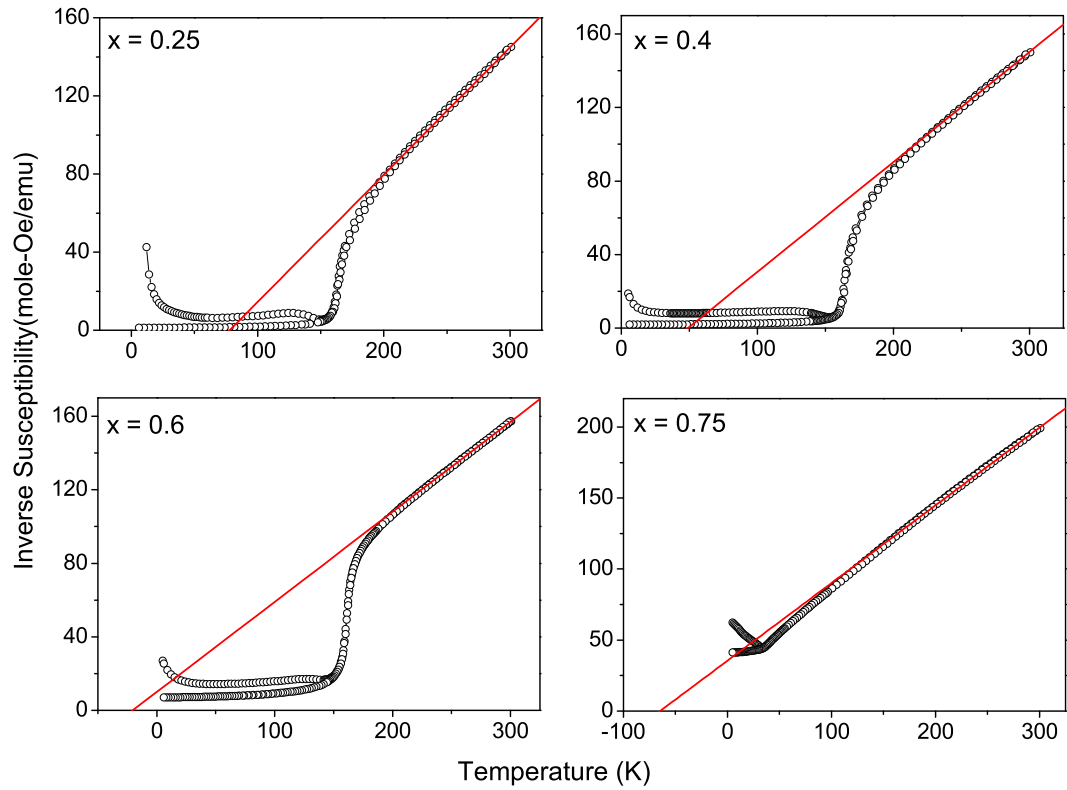


Fig. 3. Plot of inverse magnetic susceptibility (H/M) as a function of temperature calculated using magnetization data recorded in applied field of 1000 Oe in $\text{La}_{2x}\text{Sr}_{2-2x}\text{Co}_{2x}\text{Ru}_{2-2x}\text{O}_6$.

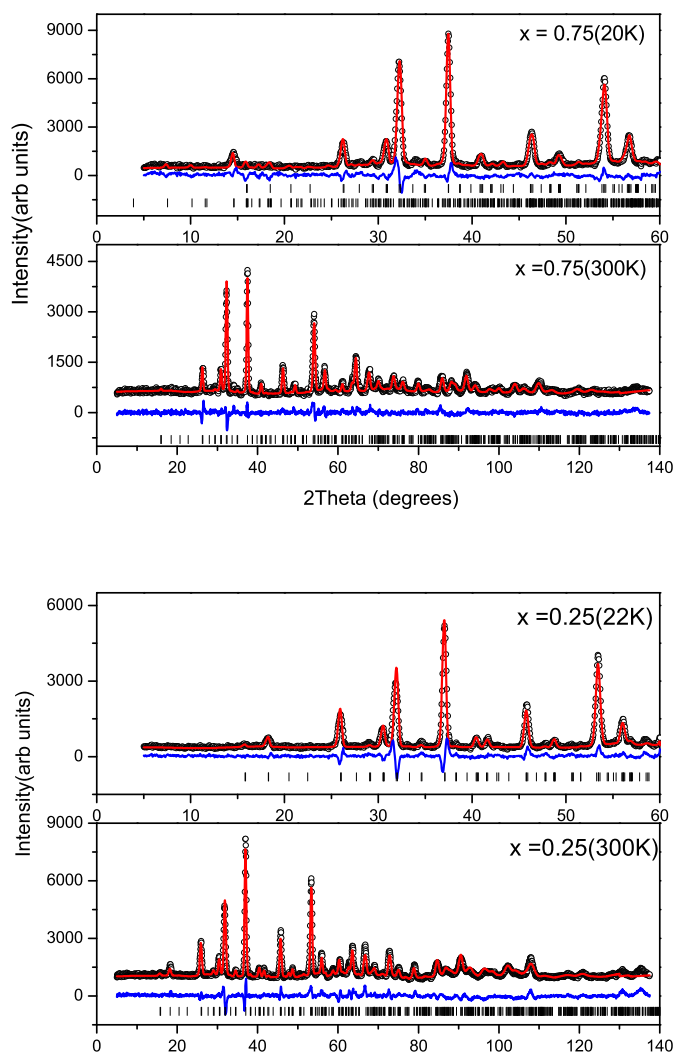


Fig. 4. Observed (circles), calculated (line) ND patterns recorded at 300K and 20K in case of $\text{La}_{2x}\text{Sr}_{2-2x}\text{Co}_{2x}\text{Ru}_{2-2x}\text{O}_6$ for $x = 0.25$ and $x = 0.75$. The data at 20K is shown in limited range for clarity. The continuous line at the bottom is the difference line between observed and calculated data.

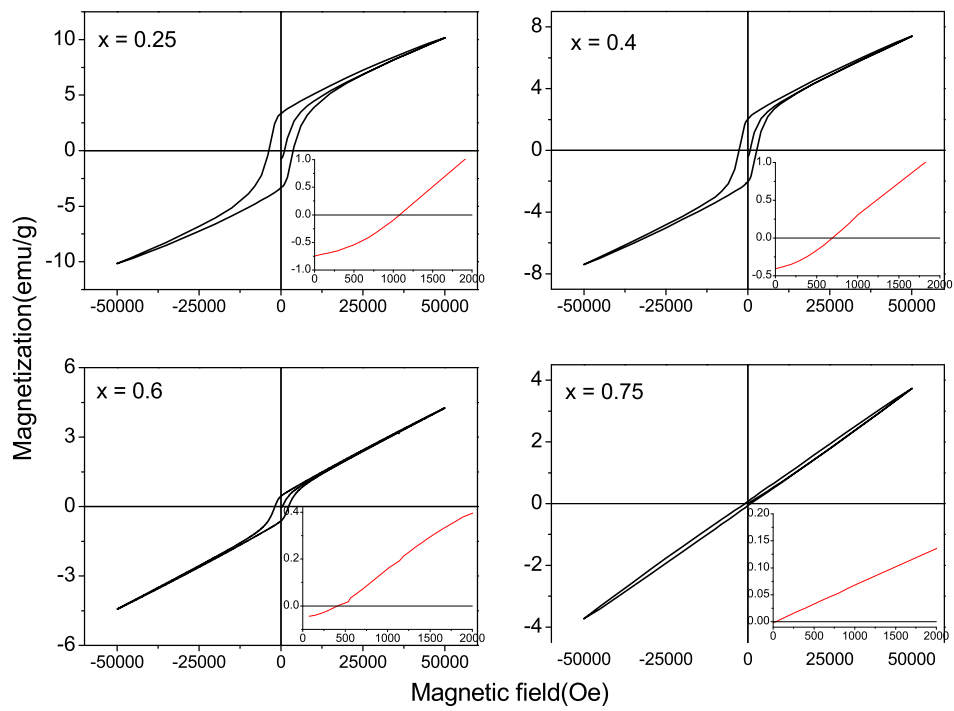


Fig. 5. Isothermal magnetization curves recorded in the field interval of $\pm 5\text{T}$ at 5K for $\text{La}_{2x}\text{Sr}_{2-2x}\text{Co}_{2x}\text{Ru}_{2-2x}\text{O}_6$.

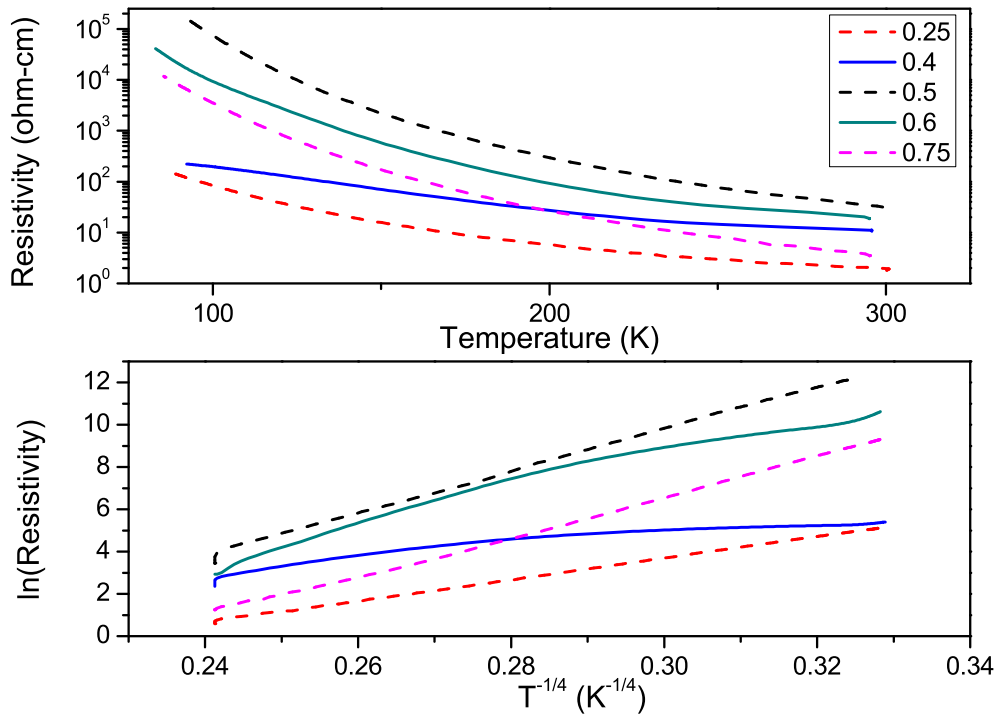


Fig. 6. Resistivity of $\text{La}_{2x}\text{Sr}_{2-2x}\text{Co}_{2x}\text{Ru}_{2-2x}\text{O}_6$ as a function of temperature (upper panel). The lower panel shows a plot of $\log \rho$ versus $T^{-1/4}$ for all compositions.

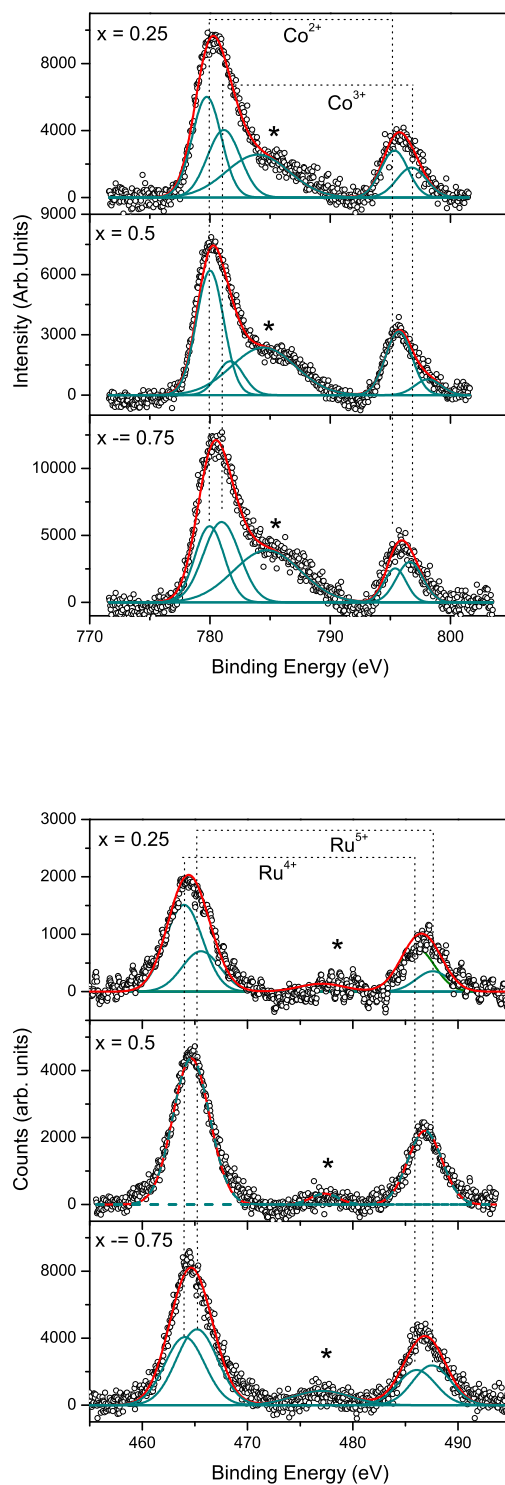


Fig. 7. Co(2p) and Ru(3p) core level spectra along with fitted curves for $\text{La}_{2x}\text{Sr}_{2-2x}\text{Co}_{2x}\text{Ru}_{2-2x}\text{O}_6$ compounds.